A D-Band LNA Exploiting Ultra-Wideband Sixth-Order Matching Networks in SiGe BiCMOS

Guglielmo De Filippi, Lorenzo Piotto, Andrea Mazzanti
Department of Electrical, Computer and Biomedical Engineering, University of Pavia, Italy

***Abstract*—Emerging applications in the Sub-THz bands need ultra-wideband amplifiers, able to cover the wide available spectrum portions with a single component. Techniques such as distributed amplifiers or stagger-tuning are commonly adopted, at the cost of power efficiency, linearity and noise figure degradation. This paper proposes a design flow for ultra-wideband matching networks with a sixth-order frequency response. The networks fit well into the layout, absorbing parasitics and embedding the interconnections for signal propagation, biasing and supply of the active stages. The networks are exploited in the design of a 3-stage D-band low-noise amplifier in a SiGe BiCMOS technology. Experiments demonstrate 105-to-175 GHz -3 dB bandwidth with 23 dB gain. The fractional bandwidth, in excess of 50%, is among the highest reported in similar frequency bands. Simultaneously, a very low noise figure, ranging from 5 dB to 6.5 dB, confirms the validity of the proposed approach to enhance the performance of mm-Wave wideband amplifiers.**

***Index Terms*—LNA, mm-Wave, broadband, matching networks, BiCMOS.**

I. Introduction

Millimeter-Wave and Sub-THz bands are gaining increasing interest, enabling high data-rate wireless communications with fiber-like transport capacity, especially for short-reach point-to-point radio backhaul links [1]. For this kind of applications, D-band ($110 \sim 170$ GHz), with favorable oxygen attenuation and a wide available bandwidth, is a promising spectrum portion.

Amplifiers are key building blocks in such systems, but the high operation frequency, close to the technology limits (f_t/f_{max}), complicates the design and penalizes the performance. Distributed amplifiers [2] have been deeply explored for high-frequency wideband amplification, but lead to large area, poor power efficiency and high noise figure [3]. A common way to extend the amplifier bandwidth is the stagger-tuning technique, where multiple tuned stages are cascaded with center frequencies purposefully misaligned such that the overall response appears broader [4]–[6]. When a high fractional bandwidth is needed, several staggered stages are required. Notably, the stage ordering is arbitrary, i.e. the stage tuned at the lowest frequency does not need to be necessarily the first stage in the chain. In [7], a three-stage amplifier is designed, and the authors place the middle frequency first, observing that this gives a flat noise figure (NF) profile. In fact, an impact on the overall amplifier performance, such as linearity and NF [8], exists. Fig. 1a depicts qualitatively this issue. The stages are characterized by center frequencies $f_{i,j,k}$. While the overall gain is independent on the stage ordering, the green and yellow curves report the overall noise figure for two different cases: lowest frequency first (i,j,k), and highest frequency first (k,j,i). Indeed, by departing from the center frequency of the first stage, the gain drops until it may be no more sufficient to suppress the noise of the subsequent stages. This determines a signal-to-noise ratio degradation in the portions of the bandwidth far from the center frequency of the first stage.

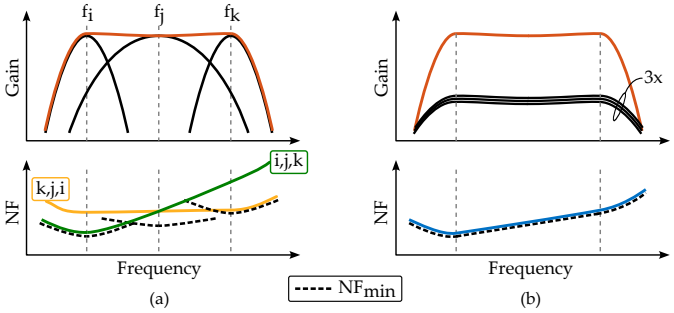

Fig. 1. Qualitative gain response (upper) and NF (lower) for a three-stage amplifier with stagger-tuning (a) and inherently broadband design (b).

This paper presents wideband amplifiers where each stage is inherently broadband, as depicted in Fig. 1b, such that the NF is minimized across all the band. The active cores are cascode stages, providing higher gain than a single common-emitter or common-base, and are loaded by high-order matching networks realized with transmission lines. Following [9], a straightforward analysis of the frequency response is provided leveraging the network similarity with the equivalent circuit of a doubly-tuned transformer. But, differently from [9], here the necessary inter-stage AC coupling capacitor is exploited to add extra singularities to the network leading to a substantial bandwidth enhancement. A three-stage low-noise amplifier (LNA) is designed and a test chip fabricated in a SiGe BiCMOS technology to validate the concept. Experimental results demonstrate 23 dB gain from 105 GHz to 175 GHz with 30 mA current consumption from a 2V supply. The corresponding fractional bandwidth is more than 50%, to the authors' knowledge the highest reported in literature for a 3-stage amplifier. Only [10] outperforms with a remarkably higher value of 77%, but the design comprises five active stages and benefits from transistors with a substantially higher f_t/f_{max}. The measured NF, between 5 dB and 6.5 dB, was demonstrated so far only by narrow-band designs.

II. Ultra-wideband Matching Networks

Cascode structures are commonly employed in multi-stage amplifiers. At high frequency, the cascode shows a relatively low input impedance but high output impedance, requiring

impedance match to rise the gain. While providing impedance scaling, the interstage network has also to feed the supply and the bias voltage to the AC-coupled stages. Moreover, in the sub-THz region, even the shortest interconnection between a transistor terminal and the topmost low-loss metal layer introduces a non-negligible reactance that should be properly absorbed by the interstage network. The topology chosen for this work is drawn in Fig. 2. L_A and L_B embed the connection to the collector of the driving stage and to the base of the following stage. Capacitors $C_{1,2}$ model the output/input parasitic capacitance of the HBTs. $L_{1,2}$ provide two convenient paths to the supply (V_{CC}) and biasing (V_b) voltage. Capacitor C_S grants the necessary AC coupling and the two $L_S/2$ segments incorporate its connections.

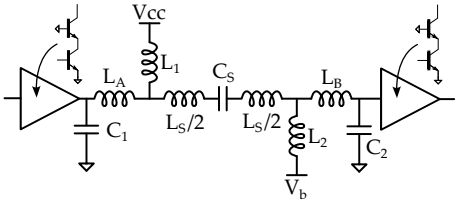

Fig. 2. Topology of the matching network employed

A rigorous study of the network in Fig. 2, in order to exploit all the available degrees of freedom, is cumbersome. Insights on components sizing and how they affect the frequency response are analyzed here following an intuitive approach to identify the network singularities and drive the design.

A. Region Around L_SC_S Resonance

From Fig. 2, the two inductors $L_S/2$ can be concentrated into a single component, L_S, as shown in Fig. 3a. For frequencies around $\omega_s = 1/\sqrt{L_s C_s}$, the series tank constituted by L_S and C_S resonates, giving ideally an AC short-circuit and leading to the simplified network of Fig. 3b, where $L_C = L_1 \,//\, L_2$. Since the T structure of L_A, L_B, L_C can be

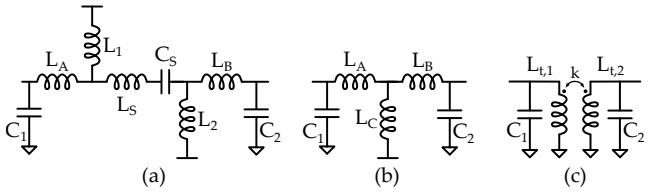

Fig. 3. Matching network rearranged (a), its simplification around ω_S (b), and equivalent circuit with a doubly-tuned transformer (c).

described by two magnetically-coupled inductors, the network is analytically equivalent to a doubly-tuned transformer with primary and secondary inductance $L_{t,1}$ and $L_{t,2}$, respectively, and magnetic coupling k, as in Fig. 3c. The relations between the parameters of the networks in Fig. 3b and Fig. 3c are:

$$L_{t,1} = L_A + L_C \qquad L_{t,2} = L_B + L_C$$
$$k = \frac{L_C}{\sqrt{(L_A + L_C)(L_B + L_C)}} \tag{1}$$

Transformers are well known for their capability of providing broadband impedance match, and this equivalence is exploited to describe the behaviour of the network of Fig. 2 in the neighborhood of ω_s. In [11], a deep study on doubly-tuned transformers was carried out. Considering Z_{in}, the impedance synthesized at the primary side, two pairs of complex-conjugate poles appear. Under the simplifying assumption that $L_{t,1}C_1 = L_{t,2}C_2 = 1/{\omega_0}^2$, their frequencies are given by:

$$\omega_{p1,2} = \frac{\omega_0}{\sqrt{1 \pm |k|}} \tag{2}$$

In addition, a pair of in-band complex zeroes appear. By properly setting the impedance transformation at these three frequencies, it is possible to achieve a broadband behaviour.

When a step-up impedance match is required (which is the case of practical interest), given a bandwidth requirement, the capacitance C_1 limits the maximum amount of impedance transformation, i.e. a higher gain can be realized only on a reduced bandwidth [11]. In the case of $C_1 = 40$ fF, Fig. 4 shows Z_{in} of the doubly-tuned transformer with 50 Ω load and a 1:2 impedance transformation ratio ($C_2 = 80$ fF and $L_{t,1} = 30$ pH, $L_{t,2} = 15$ pH, k = 0.28, implemented with $L_A = 24$ pH, $L_B = 9$ pH, $L_C = 6$ pH).

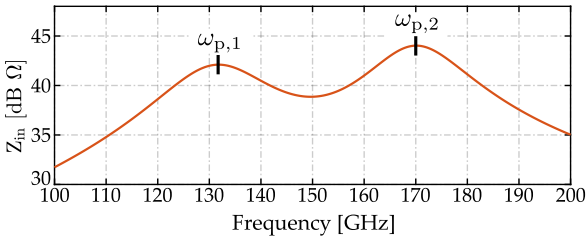

Fig. 4. Z_{in} synthesized by the doubly-tuned transformer

B. Region Far From L_SC_S Resonance

The presence of capacitor C_S and inductor L_S introduces additional singularities to the network. Regarding the zeroes on the input impedance, they can be identified by circuit inspection, noticing that a frequency exists at which the components L_1, L_S, C_S, L_2, L_B and C_2 present a capacitive impedance with reactance equal and opposite in sign to the one of L_A, thus determining a series resonance. For this reason, C_1 plays no role in these additional zeroes. The analytical expression of such singularities appears cumbersome and hardly intuitive, but it can be simplified assuming the resonance between C_2 and L_B falls at frequency sufficiently high, a condition met in practice. With this assumption, L_B is floating and the following approximated expression is found:

$$\omega_{z,s} = \sqrt{\frac{1}{C_S\left[L_2 + L_S + (L_A \,//\, L_1)\right]}} = \sqrt{\frac{1}{C_S L_{eq,z}}} \tag{3}$$

The term within square brackets at the denominator of (3) is an equivalent inductance, $L_{eq,z}$. Interestingly, (3) can be compared with (2). Replacing (1), (2) can be rewritten as:

$$\omega_{p1,2} = \sqrt{\frac{1}{C_1\left[(L_A + L_C)\left(1 \pm \frac{L_C}{\sqrt{(L_A+L_C)(L_B+L_C)}}\right)\right]}} \tag{4}$$

Again, the inductive term at the denominator of (4) may be called $L_{eq,p1}$ and $L_{eq,p2}$ with the plus and minus sign, respectively, giving:

$$\omega_{p1,2} = \sqrt{\frac{1}{C_1 L_{eq,p1,2}}} \tag{5}$$

It is evident that the additional zeroes introduced by C_S, with proper components sizing, may fall below $\omega_{p,1}$ or above $\omega_{p,2}$, thus determining bandwidth extension. For this to happen:

$$C_S > C_1 \frac{L_{eq,p1}}{L_{eq,z}} \quad \text{or} \quad C_S < C_1 \frac{L_{eq,p2}}{L_{eq,z}} \tag{6}$$

Fig. 5 reports the frequency response of Z_{in} (red curve) when L_S and C_S resonate at 177 GHz, while the additional zeroes given by (3) fall at 105 GHz, below $\omega_{p,1}$. The value of $C_S = 50$ fF is set considering practical implementation issues of such a floating MOM capacitor; going towards higher values would introduce non-negligible parasitic capacitance to ground, impairing the desired performance. L_S is set, according to (6), to 16 pH.

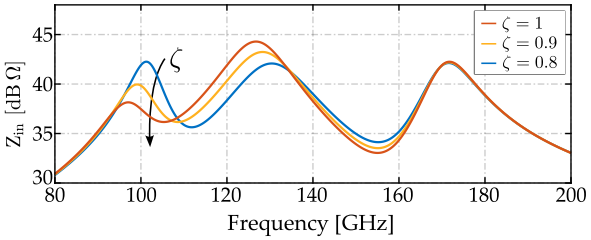

Fig. 5. Z_{in} synthesized by the network of Fig. 2. The impact of different values of ζ is reported.

A further degree of freedom not yet considered exists: only the value of $L_1 // L_2$ has been set equal to L_C, and their ratio can be expressed as $\zeta = L_2/L_1$. Interestingly, ζ controls the impedance transformation ratio in the bandwidth-extended region, with a negligible impact on the position of the singularities. To gain insight, Fig. 5 reports Z_{in} at different ζ values. While the frequencies of the singularities (hence the overall bandwidth) are marginally affected, it is possible to equalize the synthesized input impedance at the poles frequencies (ζ=0.8 gives the same Z_{in} at the three peaks).

The performance of the sixth-order matching network is finally compared (in terms of S_{21}) to the doubly-tuned transformer that gives the input impedance plotted in Fig. 4. The simulated S_{21} are reported in Fig. 6. Despite an increased in-band ripple (< 1 dB), a remarkable 30% extension of the -3dB bandwidth is evident.

III. LNA Design

The schematic of the realized three-stage LNA is reported in Fig. 7. All the transistors have an emitter area of $10 \times 0.2\,\mu m^2$ and are biased with 10 mA. $MN_{3,4,5}$ are sixth-order matching networks analyzed in the previous section, where the inductors are implemented with coplanar transmission lines in the topmost 9th metal layer. The lengths are tuned after lines

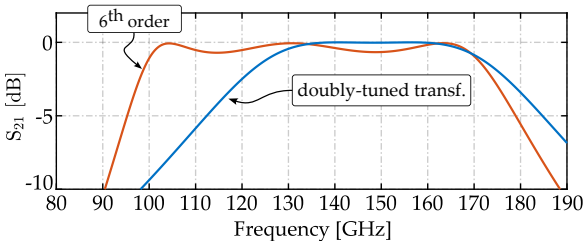

Fig. 6. S_{21} of a doubly-tuned transformer (blue) and of the network of Fig. 2 with a 1:2 impedance transformation (50 Ω load).

meandering in order to improve the area efficiency. MN_3 and MN_4 are basically identical while MN_5 embeds the GSG output pad parasitic capacitance to step-up the off-chip 50 Ω termination. MN_1 is a single-resonance matching network that transforms the 50 Ω source impedance into the optimal noise termination for Q_1. The same task is performed by MN_2 that transforms the collector impedance of Q_1 into the one that minimizes the noise figure of Q_2. Capacitors labeled as C_∞, realized with a stack of MIM and MOM components, provide an AC ground path. Low-Q multi-turn coils isolate the supply to cut uncontrolled return signal paths.

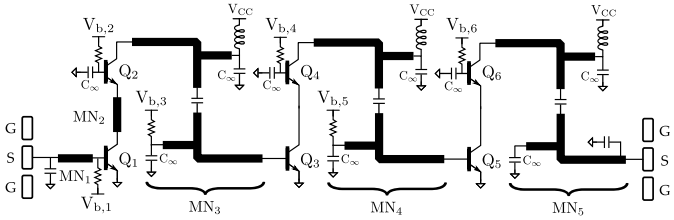

Fig. 7. Schematic of the realized LNA

IV. Experimental Results

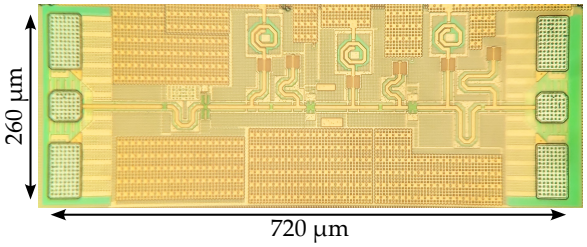

Fig. 8. Photo of the realized test-chip

The amplifier (chip photo in Fig. 8) is realized in the SiGe BiCMOS 55 nm technology of STMicroelectronics. The core area (without GSG pads) is 560 μm x 195 μm. The measurement setup allows S-parameters and NF acquisition only in the 105 - 175 GHz and 120 - 170 GHz bands, respectively. Fig. 9 plots the measured results and proves a good agreement with simulations. The lower -3 dB point is below 105 GHz, not detected by measurements due to the setup limitation. The -3 dB bandwidth, centered around 140 GHz, is (slightly) larger than 105 - 175 GHz which corresponds to a more than 50% fractional bandwidth. The NF ranges from 5 dB to 6.5 dB within the measured range.

TABLE I
COMPARISON WITH THE STATE-OF-THE-ART.

	This Work	[7]	[12]	[10]	[9]	[6]	[4]	[8]
SiGe BiCMOS Tech.	**55 nm**	55 nm	55 nm	130 nm	55 nm	130 nm	130 nm	130 nm
f_t/f_{max}	**320/370**	320/370	320/370	470/560	320/370	300/500	250/370	300/500
n. of stages	**3**	3	2	5	3	7	3	4
G_T [dB]	**23**	28.6	22.8	35	28	15.5	32.8	32.6
f_0 [GHz]	**140**	140	148	201.5	148	180	140	140
3 dB BW [GHz]	**70**	64.3	33.5	155	41	80	23.2	52
NF [dB]	**5 - 6.5**	8.8 - 10.5*	5 - 6.5	8.4 - 12	5.2 - 6.6	6.1 - 8.5	7.8 - 9.5*	4.8 - 6.1
IP_{1dB} / OP_{1dB} [dBm]	**-21.3 / 0.7**	-29.7 / -2.1	-21.8 / 0	-32 / 2	-25 / 2	-16.7 / -2.2	-28.6 / 3.2	-37.6 / -6
P_{DC} [mW]	**60**	36	40	152	60	46	39.6	28
Core Area [mm^2]	**0.109**	0.11	0.122	0.092	0.107	0.48	0.075	0.6
Frac. BW [%]	**50**	45.9	22.6	76.9	27.7	44.4	16.6	37.1
FoM	**0.204**	0.201	0.173	0.151	0.135	0.085	0.076	0.07

* simulated value

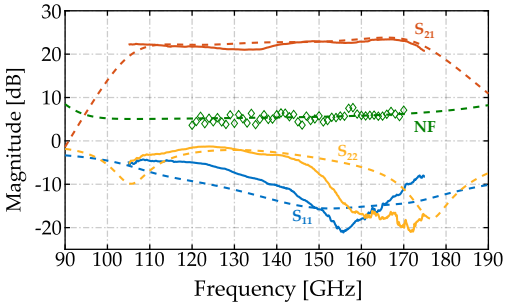

Fig. 9. Measured S-Parameters and NF compared to simulations (dashed).

The P_{1dB} of the amplifier (measured but not shown) is fairly constant and greater than 0.7 dBm (output-referred) across the bandwidth, with a peak 1.4 dBm at 150 GHz. A summary of the results is reported in Table I. Compared to prior works, the LNA demonstrates a remarkably high bandwidth, the highest among 3-stage amplifiers, with NF across the full bandwidth aligned to the best performance demonstrated only by narrow-band designs. Only [10] shows a wider fractional bandwidth which however needs more than twice the power consumption with a 5-stage design in a technology with higher f_t/f_{max}, and with a 3-to-6 dB worse NF. The figure of merit proposed in [13] is used to normalize the gain and bandwidth to the number of stages (n): $FoM = \sqrt[n]{G_T}(f_0/f_{max})^2(BW/f_0)$. The presented amplifier shows the highest FoM, similar to [7], but a 3 dB lower NF.

V. CONCLUSIONS

The drawbacks of stagger tuning, in contrast to inherently broadband designs, have been discussed, and a sixth-order transmission-line-based matching network has been proposed and analyzed for ultra-wideband amplifiers. The network can be approximated as a doubly-tuned transformer where the bandwidth is further extended leveraging the singularities introduced by the AC coupling capacitor. The concept has been applied to the design of a wideband three-stage LNA and measurements compare favorably against previous works in terms of gain-bandwidth FoM and noise figure.

ACKNOWLEDGMENT

This work received funding from the Commission of the European Union within the H2020 DRAGON project (Grant Agreement No. 955699) and KDT SHIFT project (Grant Agreement No. 1010962).

REFERENCES

[1] (2018) Point-to-Point Radio Links in the Frequency Ranges 92-114.25 GHz and 130-174.8 GHz – ECC Report 282.

[2] E. Ginzton, W. Hewlett, J. Jasberg, and J. Noe, "Distributed Amplification," *Proc. of the IRE*, vol. 36, no. 8, pp. 956–969, 1948.

[3] P. V. Testa, C. Carta, U. Jörges, and F. Ellinger, "Analysis and Design of a 30- to 220-GHz Balanced Cascaded Single-Stage Distributed Amplifier in 130-nm SiGe BiCMOS," *IEEE Journal of Solid-State Circ.*, vol. 53, no. 5, pp. 1457–1467, 2018.

[4] E. Aguilar, A. Hagelauer, D. Kissinger, and R. Weigel, "A low-power wideband D-band LNA in a 130 nm BiCMOS technology for imaging applications," in *2018 IEEE 18th Topical Meeting on Silicon Monolithic Integr. Circ. in RF Systems (SiRF), Anaheim, CA, USA*, 2018, pp. 27–29.

[5] R. Ben Yishay and D. Elad, "D-band Dicke-radiometer in 90 nm SiGe BiCMOS technology," in *2017 IEEE MTT-S Intern. Microw. Symp. (IMS), Honolulu, HI, USA*, 2017, pp. 1957–1960.

[6] Y. Mehta, S. Thomas, and A. Babakhani, "A 140–220-GHz Low-Noise Amplifier With 6-dB Minimum Noise Figure and 80-GHz Bandwidth in 130-nm SiGe BiCMOS," *IEEE Microw. and Wireless Tech. Letters*, vol. 33, no. 2, pp. 200–203, 2023.

[7] I. Petricli, H. Lotfi, and A. Mazzanti, "Analysis and Design of D-Band Cascode SiGe BiCMOS Amplifiers With Gain-Bandwidth Product Enhanced by Load Reflection," *IEEE Trans. on Microw. Theory and Techniques*, vol. 69, no. 9, pp. 4059–4068, 2021.

[8] E. Turkmen, A. Burak, A. Guner, I. Kalyoncu, M. Kaynak, and Y. Gurbuz, "A SiGe HBT D-Band LNA With Butterworth Response and Noise Reduction Technique," *IEEE Microw. and Wireless Comp. Letters*, vol. 28, no. 6, pp. 524–526, 2018.

[9] G. De Filippi, L. Piotto, A. Bilato, and A. Mazzanti, "A D-Band Low-Noise-Amplifier in SiGe BiCMOS with Broadband Multi-Resonance Matching Networks," in *2023 18th European Microw. Integr. Circ. Conf. (EuMIC), Berlin, Germany*, 2023, pp. 382–385.

[10] M. Andree, J. Grzyb, B. Heinemann, and U. Pfeiffer, "A D-Band to J-Band Low-Noise Amplifier with High Gain-Bandwidth Product in an Advanced 130 nm SiGe BiCMOS Technology," in *2023 IEEE Radio Frequency Integr. Circ. Symp. (RFIC), San Diego, CA, USA*, 2023, pp. 137–140.

[11] A. Mazzanti and A. Bevilacqua, "Second-Order Equivalent Circuits for the Design of Doubly-Tuned Transformer Matching Networks," *IEEE Trans. on Circ. and Systems I: Regular Papers*, vol. 65, no. 12, pp. 4157–4168, 2018.

[12] G. De Filippi, L. Piotto, A. Bilato, and A. Mazzanti, "A SiGe BiCMOS D-Band LNA with Gain Boosted by Local Feedback in Common-Emitter Transistors," in *2023 IEEE Radio Freq. Integr. Circ. Symp. (RFIC), San Diego, CA, USA*, 2023, pp. 133–136.

[13] D.-W. Park, D. R. Utomo, B. H. Lam, S.-G. Lee, and J.-P. Hong, "A 230–260-GHz Wideband and High-Gain Amplifier in 65-nm CMOS Based on dual-peak G_{max}-Core," *IEEE Journal of Solid-State Circ.*, vol. 54, no. 6, pp. 1613–1623, 2019.